

SUPPLEMENTARY MATERIAL

REFERENCES

41. Grimm, D., *et al.* In vitro and in vivo gene therapy vector evolution via multispecies interbreeding and retargeting of adeno-associated viruses. *Journal of virology* **82**, 5887-5911 (2008).
42. Zhang, F., *et al.* Optogenetic interrogation of neural circuits: technology for probing mammalian brain structures. *Nat Protoc* **5**, 439-456 (2010).
43. Donello, J.E., Loeb, J.E. & Hope, T.J. Woodchuck hepatitis virus contains a tripartite posttranscriptional regulatory element. *Journal of virology* **72**, 5085-5092 (1998).
44. Sohal, V.S., Zhang, F., Yizhar, O. & Deisseroth, K. Parvalbumin neurons and gamma rhythms enhance cortical circuit performance. *Nature* **459**, 698-702 (2009).
45. Gradinaru, V., *et al.* Targeting and readout strategies for fast optical neural control in vitro and in vivo. *The Journal of neuroscience : the official journal of the Society for Neuroscience* **27**, 14231-14238 (2007).

SUPPLEMENTARY METHODS

Statistical Analysis

All statistical tests were chosen based on normality of data and appropriateness of comparison to be analyzed by a particular approach. Data that were not normally distributed were either transformed to achieve normality, or analyzed with a test that does not assume normal distribution. Estimation of variance was performed by Bartlett's test for equal variance (for ANOVAs) or by an F test to compare variance (for unpaired t-tests). Variances were equal except when explicitly noted, below.

All error bars reported as s.e.m.

Supplementary Figure 3e. $n = 5$ for Chr2-eYFP group, $n = 5$ for L141 group, $n = 5$ for K75 group. One-way Type I ANOVA detected significant difference between the means: $F_{2,12} = 28.08$, <0.0001 . Chr2-eYFP group showed significant differences with both L141 and K75 groups: $p < 0.001$, Dunnett's multiple comparison tests.

Supplementary Figure 4g. $n = 8$ for fSyn-ChR2-eYFP group, $n = 5$ for intron 1+lox group, $n = 6$ for C417A group (“exon donor”), $n = 6$ for iC4A group (“intron donor”), $n = 5$ for polypyrimidine group (“intron acceptor”), $n = 4$ for iC4A;polypyrimidine group, $n = 4$ for C417A;iC4A;polypyrimidine group. One-way Type I ANOVA detected significant difference between the means: $F_{6,31} = 2.590$, $p = 0.0376$. fSyn-ChR2-eYFP and iC4A showed significant differences: $p < 0.05$, Dunnett’s multiple comparison test.

Supplementary Figure 5c. $n = 5$ for ChR2 group, $n = 5$ for N-terminus group, $n = 5$ for C-terminus group. One-way type I ANOVA detected significant differences between the means $F_{2,12} = 10.38$, < 0.0001 . ChR2 group was significantly different from both the N-terminus and C-terminus groups: $p < 0.01$ for both, Dunnett’s multiple comparison tests. Note that compared populations were heteroskedastic; post-hoc results remained significant when assessed with non-parametric Dunn’s multiple comparison test.

Supplementary Figure 9c. $n = 16$ for $C_{on}/F_{on}+MI-Cre+MI-Flp$ group, $n = 20$ for $C_{on}/F_{on}+MI-Cre$ group, $n = 20$ for $C_{on}/F_{on}+MI-Flp$ group. One-way type I ANOVA detected significant differences between the means $F_{2,53} = 26.16$, < 0.0001 . $C_{on}/F_{on}+MI-Cre+MI-Flp$ group was significantly different from both the $C_{on}/F_{on}+MI-Cre$ and $C_{on}/F_{on}+MI-Flp$ groups during the light-on epoch: $p < 0.0001$ for both, Dunnett’s multiple comparison tests. $C_{on}/F_{on}+MI-Cre+MI-Flp$ light-on was significantly different from light-off: $p = 0.0005$, Wilcoxon signed rank t -test. Note that compared populations were heteroskedastic; post-hoc results remained significant when assessed with non-parametric Dunn’s multiple comparison test.

Supplementary Figure 10. Input resistance: Data were transformed ($y = \log(y)$) to achieve normality (assessed by D’Agostino and Pearson omnibus normality test). Analysis by individual construct: One-way type 1 ANOVA detected no significant difference between the means: $F_{7,74} = 0.7256$, $p = 0.6507$. Tukey’s Multiple Comparison test of all pairs revealed no significant differences. $n = 9$ for cDIO+mCherry group, $n = 10$ for cDIO+MI-Cre group, $n = 10$ for fDIO+mCherry group, $n = 11$ for fDIO+MI-Flp group, $n = 10$ for $C_{on}/F_{on}+mCherry$ group, $n = 11$ $C_{on}/F_{on}+MI-Cre$ group, $n = 11$ for

C_{on}/F_{on}+MI-Flp group, $n = 10$ for C_{on}/F_{on}+MI-Cre+MI-Flp group. Analysis grouped by ORF configuration: One-way type 1 ANOVA detected no significant difference between the means: $F_{3,78} = 1.597$, $p = 0.1969$. Dunnett's post-tests comparing inactive configurations to active configuration are non-significant.

Capacitance: Analysis by individual construct: One-way type 1 ANOVA detected no significant difference between the means: $F_{7,74} = 1.798$, $p = 0.1004$. Tukey's Multiple Comparison test of all pairs revealed no significant differences. $n = 9$ for cDIO+mCherry group, $n = 10$ for cDIO+MI-Cre group, $n = 10$ for fDIO+mCherry group, $n = 11$ for fDIO+MI-Flp group, $n = 10$ for C_{on}/F_{on}+mCherry group, $n = 11$ C_{on}/F_{on}+MI-Cre group, $n = 11$ for C_{on}/F_{on}+MI-Flp group, $n = 10$ for C_{on}/F_{on}+MI-Cre+MI-Flp group. Analysis grouped by ORF configuration: One-way type 1 ANOVA detected no significant difference between the means: $F_{3,78} = 2.342$, $p = 0.0796$. Dunnett's post-tests comparing inactive configurations to active configuration are non-significant.

Cell counts: Chi-Squared tests of inter-condition proportions of BFP+/mCherry+ cells vs. total mCherry+ cells as counted by a blinded observer were non-significant for cDIO: $\chi^2 (1, N=125) = 0.2739$, $p = 0.6007$, non-significant for fDIO: $\chi^2 (1, N=102) = 1.497$, $p = 0.2212$, and significant for C_{on}/F_{on}: $\chi^2 (3, N=301) = 8.035$, $p = 0.0453$. Analysis grouped by ORF configuration: One-way type 1 ANOVA detected no significant difference between the means: $F_{3,12} = 2.002$, $p = 0.1675$. Dunnett's post-tests comparing inactive configurations to active configuration are non-significant. Wilcoxon Signed Rank Test (comparing each inactive condition to theoretical value of "1") was non-significant.

Supplementary Figure 11. $n = 6$ for Chr2-eYFP group, $n = 6$ for C_{on}/F_{off} group, $n = 5$ for 5' atg Δ gta group, $n = 5$ for 3' atg Δ gta group, $n = 5$ for 5'/3' atg Δ gta group, $n = 6$ for 5' atg Δ gta;3' atg Δ cta group. One-way type I ANOVA detected significant differences between the means $F_{5,27} = 8.35$, $p < 0.0001$. Bonferroni's Multiple Comparison test for differences between CY and other constructs detected significant ($p < 0.05$) differences between CY vs. C_{on}/F_{off} and CY vs. 5' atg Δ gta. Bonferroni's Multiple Comparison test for differences between C_{on}/F_{off} and other constructs detected significant

($p < 0.05$) differences between C_{on}/F_{off} vs. 5'/3' atg Δ gta and C_{on}/F_{off} vs. 5' atg Δ gta; 3' atg Δ cta group.

Hippocampal neuron culture and calcium phosphate transfections

Primary cultured hippocampal neurons were prepared from P0 Spague-Dawley rat pups (Charles River). The CA1 and CA3 regions were isolated, digested with 0.4 mg/mL papain (Worthington, Lakewood, NJ), and plated onto 12 mm glass coverslips precoated with 1:30 Matrigel (Beckton Dickinson Labware, Bedford, MA) in a 24-well plate. Cultures were maintained in a 5% CO₂ humid incubator with Neurobasal-A medium (Invitrogen Carlsbad, CA) containing 1.25% FBS (Hyclone, Logan, UT), 4% B-27 supplement (Gibco, Grand Island, NY), 2 mM Glutamax (Gibco), and FUDR (2 mg/ml (Sigma, St. Louis, MO).

Day 6-10 old neurons at a density of about 75,000 cells/well were used for all transfections. MEM was prewarmed in a 37 C water bath (30 minutes prior to start). In an 1.5 ml eppendorf tube the DNA + CaCl₂ mix for each 12 mm coverslip was prepared as follows: 1.5-3 μ g endotoxin-free DNA + 1.875 μ l 2M CaCl₂ (250 mM final) + Sterile Water to 15 μ l total volume. 15 μ l 2X sterile filtered HBS (in mM 50 HEPES, 1.5 Na₂HPO₄, 280 NaCl, pH 7.05 with NaOH) was added to each mix, pipetted to mix and incubated 20 minutes at room temperature. 15 minutes into the incubation, the media from the cultured neurons was replaced with 400 μ l prewarmed MEM, while saving the neuronal media. The DNA + CaCl₂ + HBS mix was added drop-wise to each well and the cultures were placed in a 37 C incubator for 45-60 minutes. MEM and saved neuronal media was kept warm in a 37 C water bath. Each well was washed with 1 ml MEM x 3, making sure that the coverslip did not dry out during the wash then replaced with saved neuronal media and returned to the incubator. Expression is generally seen at 20-24 hours.

mRNA isolation and cDNA synthesis

HEK293FT cells at 90% confluence were transfected with endotoxin free DNA using lipofectamine 2000 (Invitrogen) following manufacturer protocol. Five days post-

transfection, RNA extraction was performed using reagents from RNeasy Mini Kit (Qiagen). Cells were disrupted with lysis buffer and homogenized using QiaShredder homogenizer columns. Combined first strand cDNA/PCR using SuperScript III One-Step RT-PCR System (Invitrogen) was performed with the following reaction conditions (°C): 45 x 30 min, 94 x 2 min, 40 cycles of 94 x 15 sec, 45 x 30 sec, 68 x 1 min, ending with 68 x 5 min using various combinations of primers below as indicated. The PCR product was gel purified and sequenced to determine splice junctions.

Exon	Strand	Sequence (5'-3')
1	F	agtggctgctcactgtcct
2	R	gcacaatccaagacaaaagaag
2	F	agctggacggcgacgtaaac
3	R	aagtcgtgctgcttcatgtg

Mutagenesis

Intron mutations were introduced using QuikChange Lightning II Mutagenesis Kit (Agilent) with the following primers:

	Forward Primer (5'-3')	Reverse Primer (5'-3')
ChR2 C417A	ctgagcaacctcacaggtacgtgcgggg	ccccgacacgtacctgtgaggtgctcag
intron 1 C4A	caacctcaccggaagtgtcggggttgc	gcaaccccgacacttaccggtgaggttg
intron 1 polypyrimidine tract	gtgcttatgactctatttcttctctttaggcctg agcaacgacta	tagtcggtgctcaggcctaaagagaagagaa atagagtcataagcac

Virus production

AAV-2/5

Adeno-associated virus (AAV) serotype 2/5 was produced by the University of North Carolina Chapel Hill Vector Core.

AAV-DJ

AAV-DJ serotype was produced by the Stanford Neuroscience Gene Vector and Virus Core. In brief, AAV-DJ⁴¹ was produced by transfection of AAV 293 cells (Agilent) with three plasmids: an AAV vector expressing the recombinase-dependent construct, AAV helper plasmid (pHELPER; Agilent) and AAV rep-cap helper plasmid (pRC-DJ, gift from M. Kay, Stanford University). At 72 h post-transfection, the cells were collected and lysed by a freeze-thaw procedure. Viral particles were then purified by an iodixanol step-gradient ultracentrifugation method. The iodixanol was diluted and the AAV was concentrated using a 100-kDa molecular mass cutoff ultrafiltration device. Genomic titer was determined by quantitative PCR. Infectious titers were determined on 293 cells and/or primary neurons.

AAV-10

AAV-10 was packaged via pseudotyping in AAV 10 capsid proteins in the laboratory of Dr. Caroline Bass at the University at Buffalo, using the standard triple transfection technique.

Lentivirus

Lentivirus was prepared as described previously⁴² using triple transfection of HEK293 cells with VSVG, pDelta, and payload construct. For rapid construct prototyping, small batches were made from single 225cm² plates.

HSV

Long Term Herpes Simplex Virus (LT-HSV) was created by modification of Short Term HSV (ST-HSV) as follows: The promoter was changed from hCMV-E11 to EF1 α , polyadenylation (pA) signal changed from SV40 late pA to SV40 early pA, and the 692

bp woodchuck hepatitis virus post-transcriptional response element⁴³ was added. LT-HSV vectors are available from the Massachusetts Institute of Technology Viral Gene Transfer Core.

Mouse Genotyping protocols:

Transgene	Primers (5' -> 3')	PCR (°C)	Band Size (bp)
Cre	F: AAGAACCTGATGGACATGTTTCAGGGATCG R: CCACCGTCAGTACGTGAGATATCTTTAACC	94 x 3 min ----- 94 x 45 sec 65 x 30 sec 72 x 90 sec 30 times ----- 72 x 10 min	550
Flp	F: GACAAGGGCAACAGCCACAGCA R: TTGCTGATGGGGTCGTAGGCGTAG	95 x 3 min ----- 94 x 10 sec 55 x 30 sec 68 x 1 min 10 times ----- 94 x 15 sec 55 x 30 sec 68 x 80 sec 25 times ----- 68 x 7 min	707

Stereotactic injections

Stereotactic viral injections were carried out as previously described⁴⁴. Briefly, mice induced and maintained on isoflurane anesthesia were placed in a stereotactic frame (Kopf Instruments) and the head leveled using bregma and lambda skull landmarks. Craniotomies were performed so as to cause minimal damage to cortical tissue using a hand drill. Injections were made using a 10µL syringe and 35g beveled needle (World

Precision Instruments). 1000 nl of viral suspension was infused at a rate of 100-150 nl/min at the following coordinates (mm):

	A/P	M/L	D/V
Medial Prefrontal Cortex	+1.80	0.35	-2.85
CA1 anterior	-1.75	1.00	-1.15
CA1 medial	-2.50	1.60	-1.3
CA1 posterior	-2.80	2.00	-1.3
Dentate Gyrus	-2.5	1.6	-2.1
Nucleus Accumbens	+1.2	0.75	-4.5
Ventral Tegmental Area (dorsal)	-3.3	0.4	-4.2
Ventral Tegmental Area (ventral)	-3.3	0.4	-4.7

Histology

Following virus injection, mice were transcardially perfused with 20 mL ice-cold PBS followed by 20 mL 4% paraformaldehyde (PFA). After an overnight post-fix in PFA, brains were equilibrated in sterile 30% sucrose/PBS for at least 24 hours. Tissue was sectioned at 40 μ m using a frozen microtome, stained, and mounted with PVA-DABCO (Sigma). Images were obtained on a Leica confocal microscope using 5x, 40x, and 63x objectives. All secondary antibodies (Jackson ImmunoResearch) were used at 1:500. Primaries are as follows:

	Manufacturer	Part Number	Species	Concentration
2a	Millipore	ABS31	Rabbit	1:500
Parvalbumin	Sigma	P3088	Mouse	1:500
Somatostatin	Santa Cruz	Sc-7819	Goat	1:500
Tyrosine Hydroxylase	Aves	TYH	Chicken	1:500
Streptavidin-350	Invitrogen	S-11249		1:500

***In vivo* optrode recordings**

In vivo recordings of recombinase-induced ChR2 expression in hippocampus were performed as described previously⁴⁵. Clampex software was used for both recording signals and controlled 473nm (Crystallaser, Inc.) 100mW solid-state laser diode source coupled to the optrode. Neuronal activity was evoked by 1.5 s of pulsed (10Hz, 5ms pulse-width) 473 nm light.

Culture Electrophysiology

Primary hippocampal neurons produced, plated, and transfected as above were identified for recording by fluorescent protein expression. Recordings were obtained in Tyrode's medium ([mM] 150 NaCl, 4 KCl, 2 MgCl₂, 2 CaCl₂, 10 D-glucose, 10 HEPES, pH 7.35 with NaOH) supplemented with TTX (Tocris 1 μM), APV (Tocris 10 μM), and/or CNQX (Tocris 25 μM) as indicated with a standard internal solution ([mM] 130 KGluconate, 10 KCl, 10 HEPES, 10 EGTA, 2 MgCl₂, pH 7.3 with KOH) in 3-5 MOhm glass pipettes. Filtered light from a xenon lamp (DG-4 Sutter Instruments) was coupled to the fluorescence port of the microscope (Leica DM-LFSA). The ChR2 stimulation filter (473 nm Semrock) had approximately 20 nm bandwidth.

Slice Electrophysiology

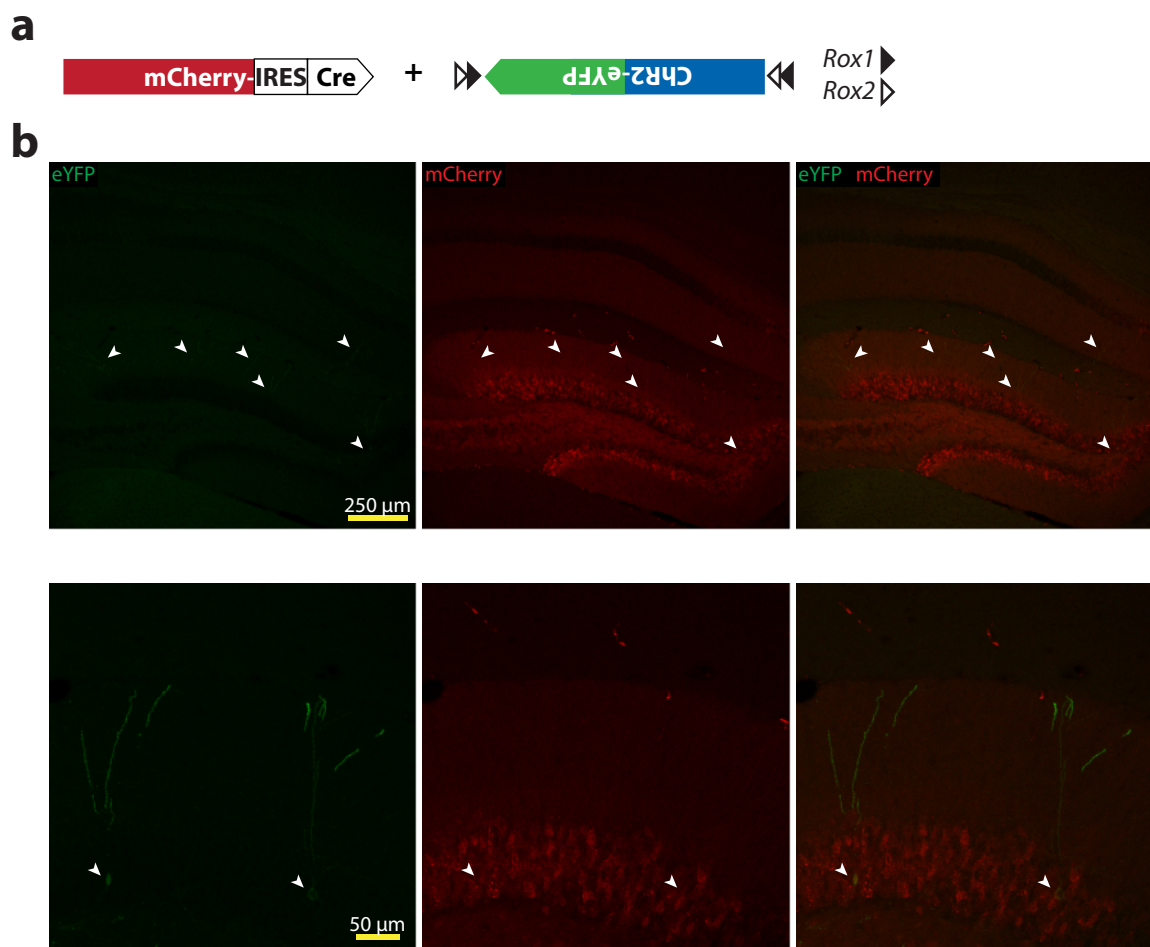
Coronal slices (300 μm) from mice previously injected with virus were prepared after intracardial perfusion with ice-cold, sucrose-containing artificial cerebrospinal fluid (ACSF) in mM: 85 NaCl, 75 sucrose, 2.5 KCl, 25 glucose, 1.25 NaH₂PO₄, 4 MgCl₂, 0.5 CaCl₂, and 24 NaHCO₃. Slices were incubated for 1 hr at 32-34°C, and then transferred to an oxygenated standard ACSF solution at room temperature (in mM): 123 NaCl, 3 KCl, 26 NaHCO₃, 2 CaCl₂, 1 MgCl₂, 1.25 NaH₂PO₄, and 11 glucose, with synaptic transmission blockers D(-)-2-amino-5-phosphonovaleric acid (APV; 25 μM), 2,3-dihydroxy-6-nitro-7-sulfamoyl-benzo[f]quinoxaline-2,3-dione (NBQX; 10 μM), and gabazine (10 μM). Electrophysiological recordings were performed at 32-34°C. Slices were visualized with an upright microscope (BX61WI, Olympus) equipped with a 40X water-immersion objective and infrared differential interference contrast (IR-DIC) optics. Individual neuron recordings were obtained after identifying fluorescent protein

expression under constant ACSF perfusion. Filtered light from a Spectra X Light engine (Lumencor) was coupled to the fluorescence port of the microscope and used both to view fluorescence and deliver light pulses for opsin activation. Power density of the blue light (475/28 nm) was 5 mW/mm^2 , measured with a power meter (ThorLabs). Whole-cell recordings were obtained with patch pipettes pulled from borosilicate glass capillaries (Sutter Instruments) with a horizontal puller (P-2000, Sutter Instruments) and contained the following internal solution (in mM): 125 K-gluconate, 10 KCl, 10 HEPES, 4 Mg_3ATP , 0.3 NaGTP, 10 phosphocreatine, 1 EGTA, 8 biocytin. $1 \mu\text{M}$ tetrodotoxin was added to the external recording solution when necessary to eliminate escape spikes for peak photocurrent measurements. Recordings were made using a MultiClamp700B amplifier (Molecular Devices). Signals were filtered at 4 kHz and digitized at 10 kHz with a Digidata 1440A analog–digital interface (Molecular Devices). pClamp10.3 software (Molecular Devices) was used to record and analyze data. Peak and steady-state photocurrents were measured from a 1 s light pulse in voltage-clamp mode. Series resistances were carefully monitored and recordings were not used if the series resistance changed by a large magnitude (by $>20\%$) or reached $25 \text{ M}\Omega$. Input resistance and capacitance were both calculated from the response to 10 mV voltage steps in voltage clamp, using steady-state current amplitude and recovery from the capacitive transient, respectively.

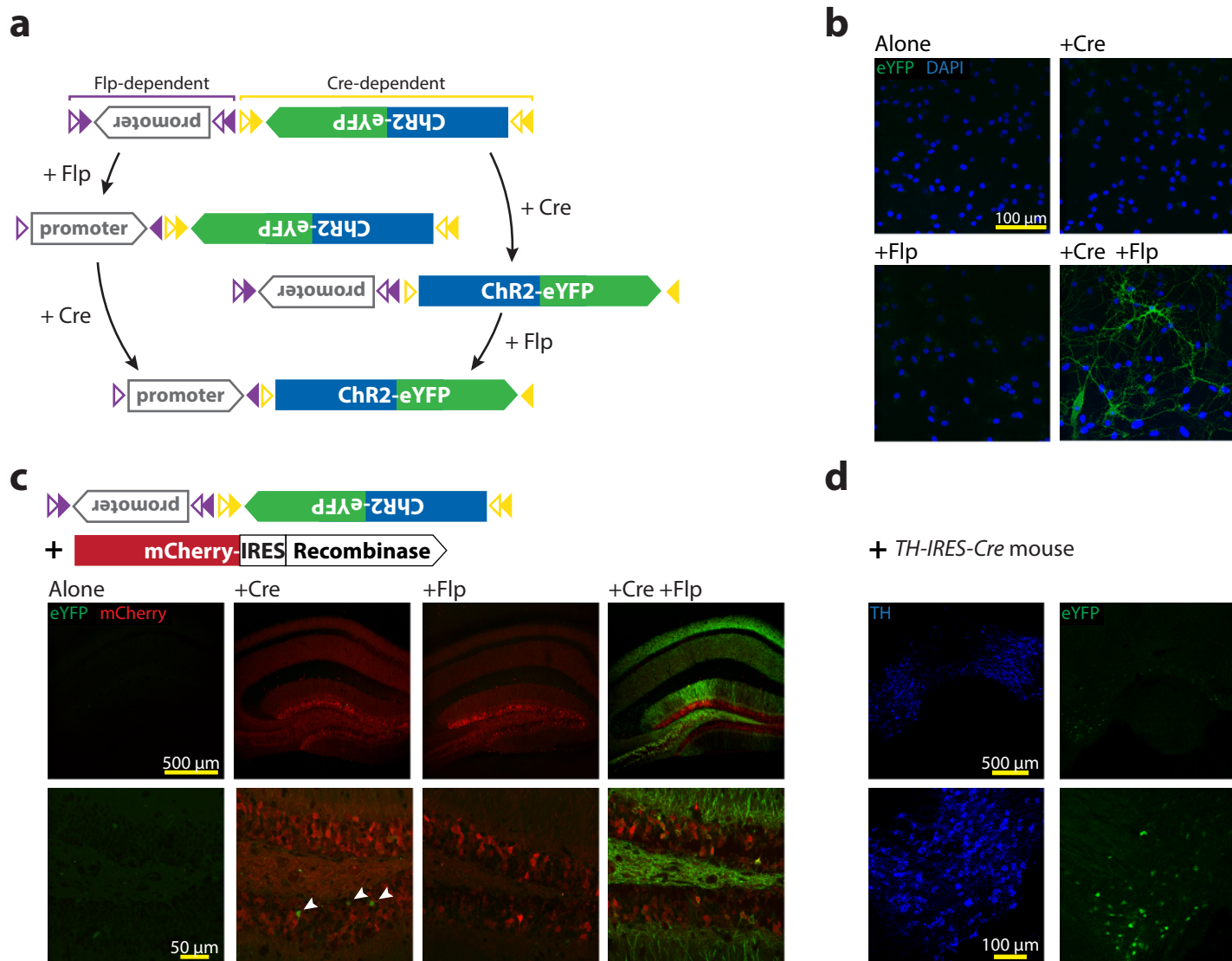
Slice histology

300 μm acute slices used in electrophysiology recordings with biocytin filled recording pipettes were prepared in a two-step process. Slices were first processed for immunohistochemistry by post-fixing in 4% PFA with 0.2% picric acid in 0.1M phosphate buffer (in mM 80 Na_2HPO_4 , 20 NaH_2PO_4) for at least one day following recording, washed in 0.1M Phosphate Buffer, and incubated overnight at 4C with primary antibodies diluted in 0.05M TBS (in mM 42 Trizma HCl, 8 Trizma Base, 154 NaCl) with 0.5% Triton X-100. The next day, slices were washed in 0.1M TBS, incubated in secondary at RT for 3 hours, washed in 0.1M PB, and mounted using Vectashield (Vector Laboratories). After imaging, slices were processed for bright-field morphological analysis.

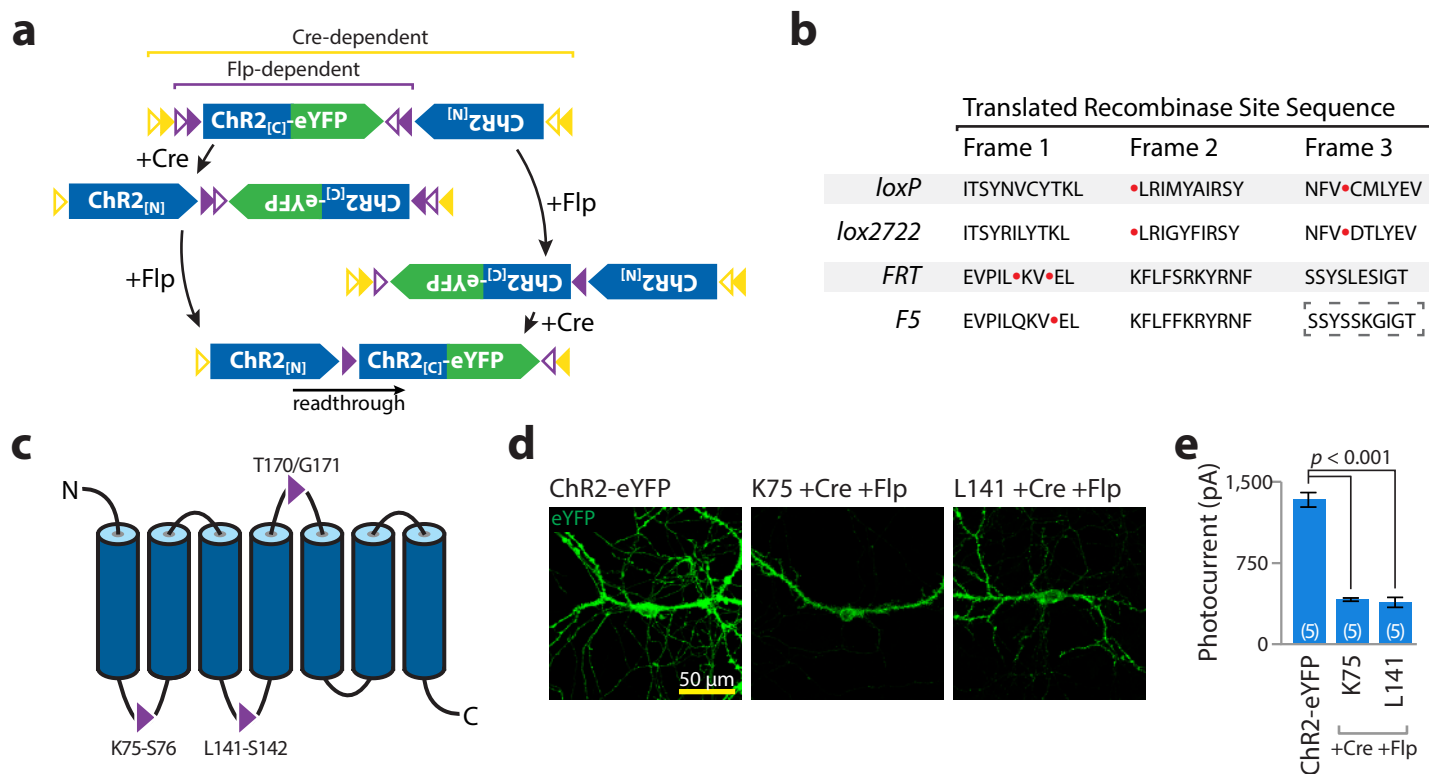
For morphological analysis of axonal and dendritic arbors, slices were unmounted, washed in 0.1M PB, treated with 1% hydrogen peroxide to extinguish endogenous peroxidases, washed again, treated with 50-70-50% EtOH steps, washed, processed to form Avidin-DH/Biotin Complexes (Vectastain ABC kit, Vector Laboratories) in 0.05M TBS with 0.5% Triton X-100 overnight at 4C. The next day, after washing in 0.1M PB, slices were reacted with 3,3'-diaminobenzidine tetrahydrochloride (0.015%, DAB Substrate Kit for Peroxidase, Vector Laboratories), washed, dehydrated, cleared with Citrisolv (Fisherbrand), and mounted (DPX, Electron Microscopy Sciences). Morphology was resolved by examining shape and location of cell body, dendrites, and axon; reconstructions rendered with StereoInvestigator (MBF) and Photoshop (Adobe).



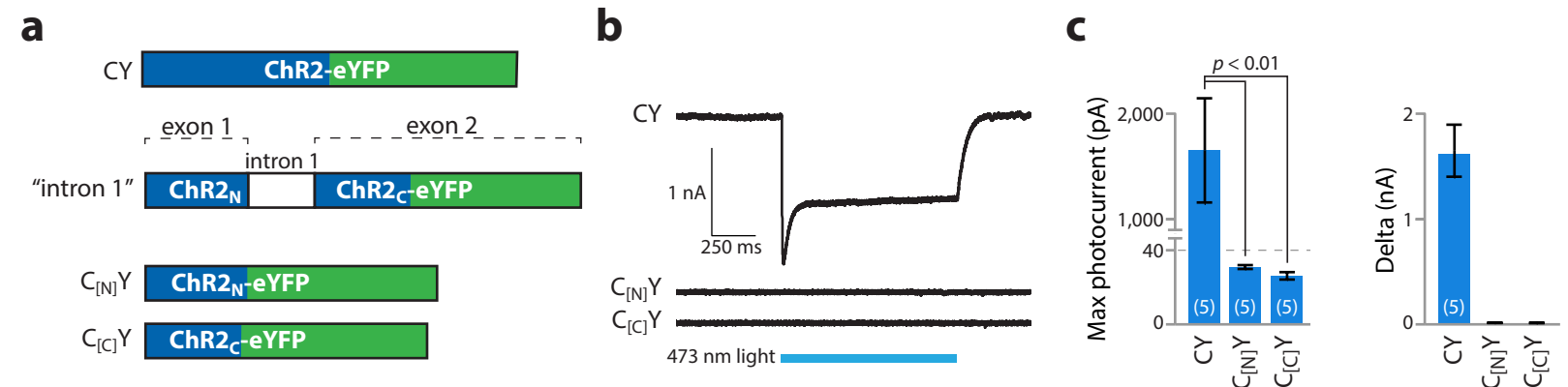
Supplementary Figure 1. *In vivo* activation of dDIO by Cre recombinase. **a)** Wild-type mice were co-injected with one AAV containing Cre and mCherry and a second containing Dre recombinase-dependent dDIO-ChR2-eYFP. **b)** dDIO-ChR2-eYFP activity is seen in mCherry-IRES-Cre expressing cells (arrowheads), indicating activation of dDIO-ChR2-eYFP by Cre.



Supplementary Figure 2. Recombinase/viral strategies for intersectional genetic targeting: promoter and ORF approach. **a)** Schematic of independent directional control of promoter (Doublefloxed Inverted Promoter; ‘DIP’) and ORF (DIO) by Flp and Cre, respectively. The promoter and ORF are in the reverse orientation. Flp activity reverses the direction of the promoter, while Cre activity reverses the direction of the reading frame. The action of both Cre and Flp will position the promoter and ORF in the correct orientation. **b)** DIP/DIO-ChR2-eYFP is only expressed in cultured neurons in the presence of both Cre and Flp. **c)** To examine function of this strategy *in vivo*, DIP/DIO-ChR2-eYFP and mCherry-tagged recombinases were injected as indicated in wild type animals. Robust expression was observed in the triple-injection condition, while no expression was observed when DIP/DIO was injected alone or with Flp. Sparse cells were observed when co-injected with Cre (arrowheads). Imaging settings were individually optimized for each image. **d)** Further examination of this leak was investigated by injection of DIP/DIO-ChR2-eYFP into the VTA of *TH-IRES-Cre* animals. Extensive expression throughout the VTA was observed, validating observed leak in dual DIP/DIO + Cre injection in **c**.

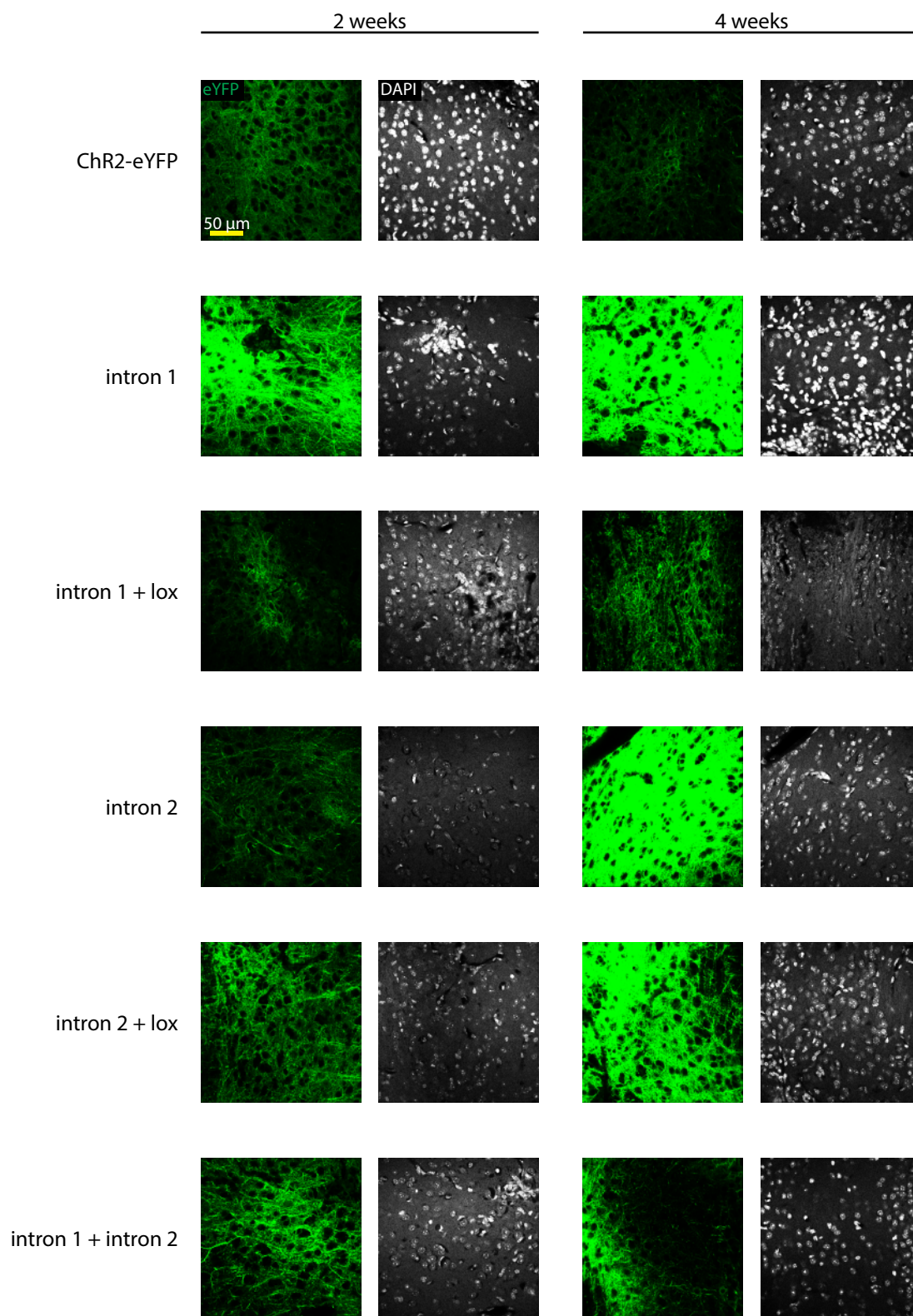


Supplementary Figure 3. Recombinase/viral strategies for intersectional genetic targeting: nested recombinase approach. **a)** Schematic of independent directional control of complete ORF and N-terminal of ChR2-eYFP with nested Cre and Flp DIO. The action of Cre and Flp position the entire reading frame in the correct orientation, leaving a single recombinase recognition site in-frame within the coding sequence of ChR2. **b)** Translation of four recombinase recognition sites in three reading frames. Red dots indicate STOP codons, dashed box indicates site/reading frame used in construct (see methods for criteria). **c)** Three loop insertion sites used for *F5* recombinase site. **d,e)** Primary neurons triple transfected with Cre, Flp, and ChR2-eYFP with or without the indicated insertion site (K75 or L141) expressed eYFP (**d**), but photocurrents were greatly diminished when reading frame retains the *F5* site (**e**).



Supplementary Figure 5. ChR2 exons do not encode functional activity in isolation. a) Schematics: ChR2-eYFP without and with an intron, and truncated ChR2 constructs. Note ChR2[N] and ChR2[C] correspond to fragments in exon 1 and exon 2, respectively, in constructs with introns. ChR2[C] has a one-base addition at the 5' terminal to maintain the correct reading frame (construct does not express without this manipulation; data not shown). **b)** Representative whole-cell voltage-clamp recordings from indicated constructs illustrating light response only when the entire ChR2 sequence is present. **c)** Max stimulation photocurrent and delta between baseline and stimulation epochs for ChR2, ChR2[N], and ChR2[C]. One-way type I ANOVA detected significant differences between the maximum photocurrent means ($F_{2,12} = 10.38, <0.0001$); ChR2 group was significantly different from both the N-terminus and C-terminus groups ($p < 0.01$ for both, Dunnett's multiple comparison tests). Average change in peak recorded photocurrents from ChR2, ChR2[N], and ChR2[C] were 1614 ± 500 pA, -0.9 ± 2.8 pA, and 5.6 ± 3.0 pA ($n=5$ for each construct).

Supplementary Figure 6 - INTRSECT: single-component targeting of cells using multiple-feature Boolean logic



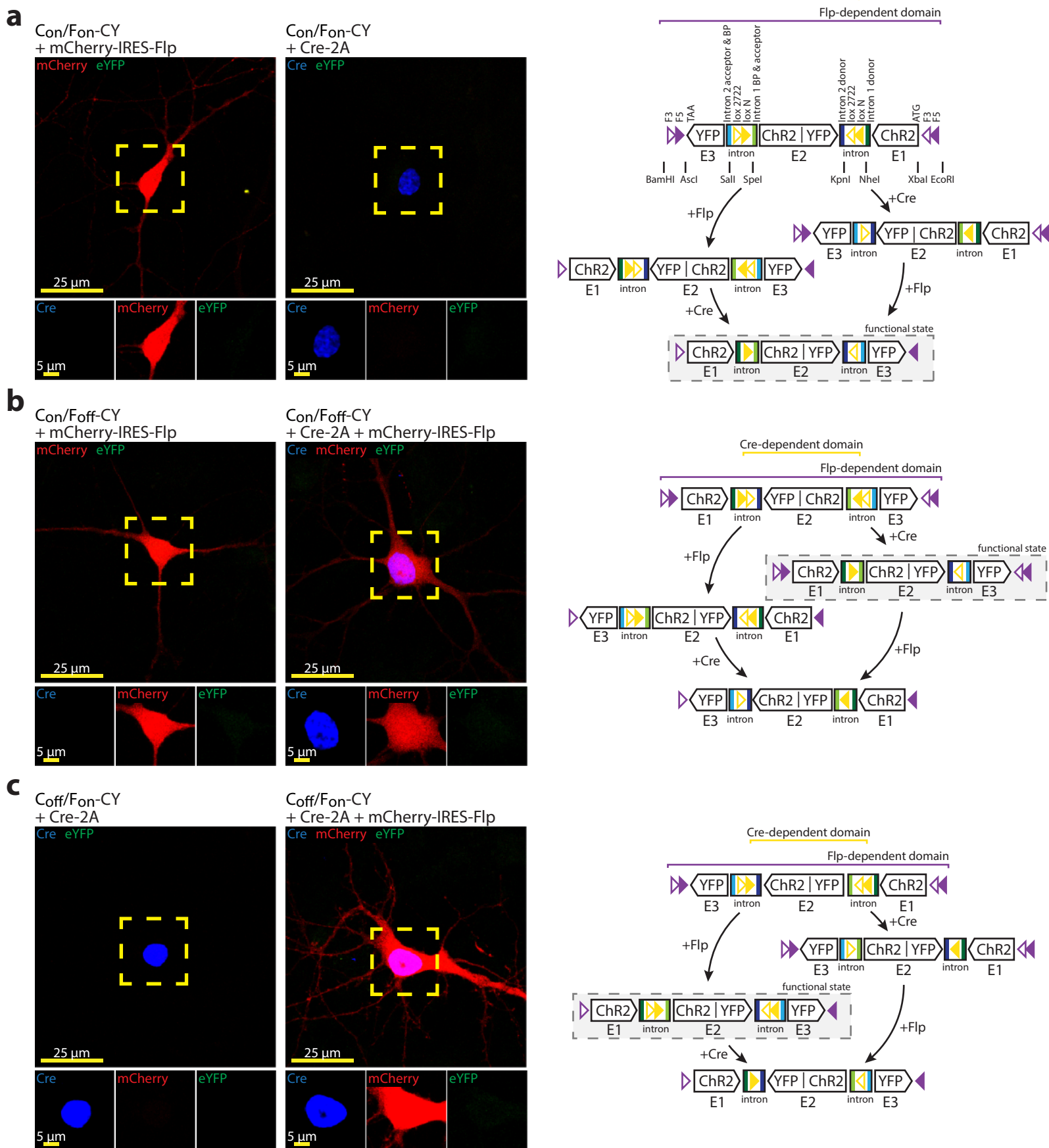
Supplementary Figure 6. Chr2-eYFP is expressed in vivo after addition of introns with or without sequence addition. Lentivirus made from Chr2-eYFP with various intron additions to the reading frame (nomenclature as in Figure 2) driven by human Synapsin promoter was injected into the medial prefrontal cortex of mice bilaterally. Expression was assayed at 2 or 4 weeks after injection. Expression was observed as early as 1 week post-infection (data not shown); all constructs expressed at 2 and 4 week time points, indicating successful intron splicing.

Supplementary Figure 7 - INTRSECT: single-component targeting of cells using multiple-feature Boolean logic

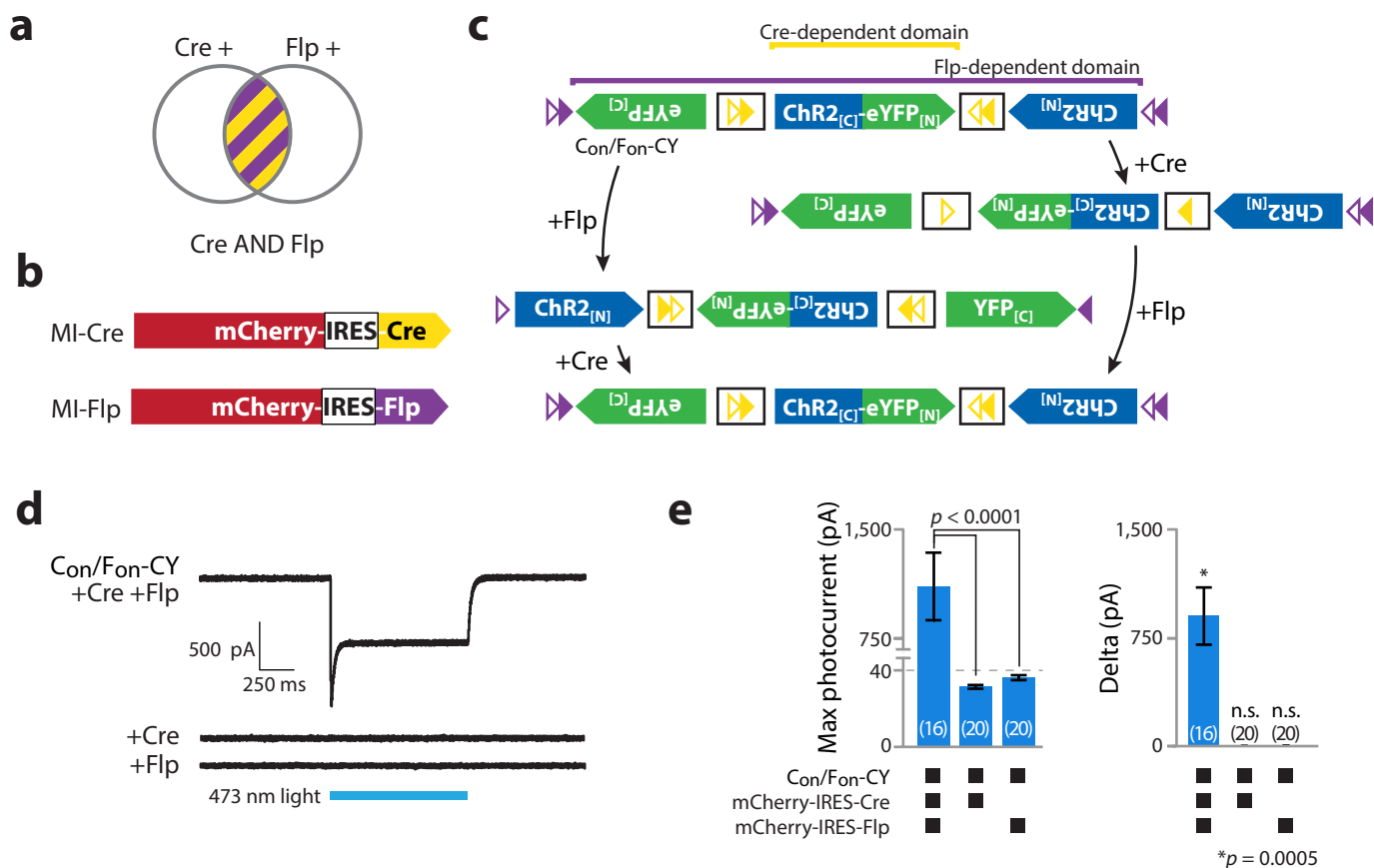
		5' palindrome	spacer	3' palindrome
Cre recognition sites	<i>LoxP</i>	ATAACTTCGTATA	ATGTATGC	TATACGAAGTTAT
	<i>Lox2722</i>	ATAACTTCGTATA	GGATACTT	TATACGAAGTTAT
	<i>LoxN</i>	ATAACTTCGTATA	GTATACCT	TATACGAAGTTAT
Dre recognition sites	<i>Rox1</i>	TAACTTTAAATAAT	GCCA	ATTATTTAAAGTTA
	<i>Rox2</i>	TAACTTTAAATAAT	GTCC	ATTATTTAAAGTTA
Flp recognition sites	<i>FRT</i>	GAAGTTCCTATTC	TCTAGAAA	GTATAGGAAGTTC
	<i>F5</i>	GAAGTTCCTATTC	TTCAAAG	GTATAGGAAGTTC
	<i>F3</i>	GAAGTTCCTATTC	TTCAAATA	GTATAGGAAGTTC
SCre recognition sites	<i>SLoxP</i>	CTCGTGTCCGATA	ACTGTAAT	TATCGGACATGAT
	<i>SLox2722</i>	CTCGTGTCCGATA	AGTGATT	TATCGGACATGAT
VCre recognition sites	<i>VLoxP</i>	TCAATTTCTGAGA	ACTGTCAT	TCTCGGAAATTGA
	<i>VLox2722</i>	TCAATTTCTGAGA	AGTGCTT	TCTCGGAAATTGA

■ Base differs from canonical site

Supplementary Figure 7. Recombinase recognition sites used for integrated intron and recombinase targeting. Recognition site sequences for Cre, Dre, Flp, SCre, and VCre. Red indicates nucleotides that differ from the wild type site.



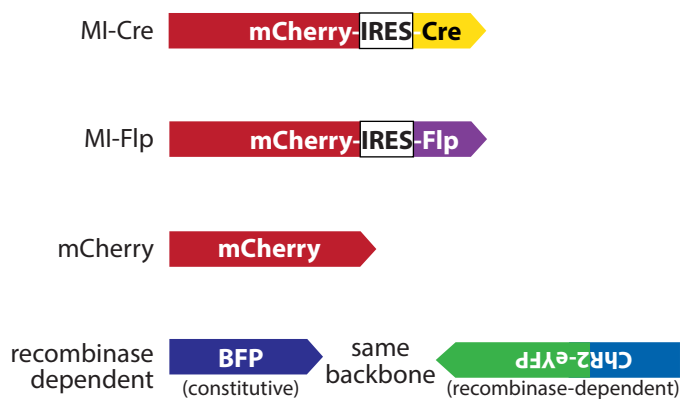
Supplementary Figure 8. Detailed molecular map of integrated intron and recombinase targeting strategies with exemplar non-functional intermediates. ChR2-eYFP in Con/Fon (a), Con/Foff (b), and Coff/Fon (c) configurations transfected with Cre (blue) and Flp (red) as indicated (left). No eYFP expression is noted as combinations of recombinases used here do not fulfill the criteria for activation, instead driving ChR2-eYFP to a non-functional configuration (right). For completeness, intronic donor and acceptor sites for both introns as well as all recombinase recognition sites are tracked through each recombinase dependent state. Functional states indicated by dashed box.



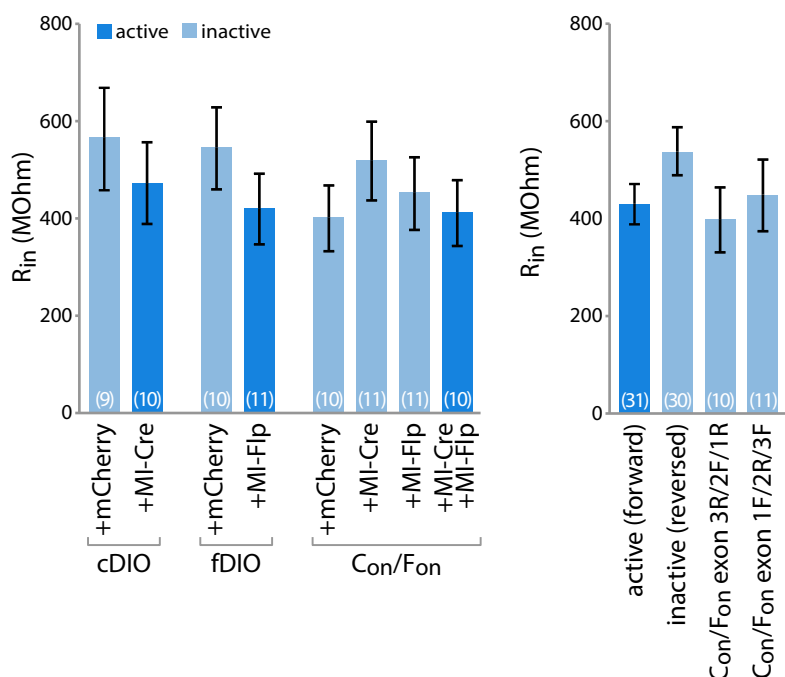
Supplementary Figure 9. Con/Fon-ChR2-eYFP does not generate photocurrents in the absence of either Cre or Flp.

a,b) Schematic of cells targeted by Con/Fon ChR2-eYFP (**a**) and mCherry-tagged bicistronic constructs (**b**) used for recombinase expression. **c)** ChR2-eYFP is only active after the independent activity of both Cre and Flp recombinase, as no intermediate generated after the isolated activity of a single recombinase generates a coherent open reading frame. **d)** Exemplar voltage clamp recordings from neurons transfected with indicated constructs and patched based only on the expression of mCherry, without examination of eYFP expression. **e)** Max stimulation photocurrent and delta between baseline and stimulation epochs for neurons selected from only mCherry expression. Mean peak photocurrents were 1103.7 ± 235.9 pA for triple transfection (n=16), 27.0 ± 0.8 pA for Cre co-transfection (n=20), and 31.2 ± 1.1 pA for Flp co-transfection (n=20). 14/16 neurons patched in triple transfection condition, 0/20 in Cre only, and 0/20 in Flp only, generated photocurrents more than 2 standard deviations larger than baseline noise. One-way type I ANOVA detected significant differences between the maximum photocurrent means ($F_{2,53} = 26.16, <0.0001$); Con/Fon+MI-Cre+MI-Flp group was significantly different from both the Con/Fon+MI-Cre and Con/Fon+MI-Flp groups during the light-on epoch ($p < 0.0001$ for both, Dunnett's multiple comparison tests). Average change in peak recorded photocurrents from +Cre/+Flp, +Cre alone, and +Flp alone were 1071 ± 236 pA, -2.7 ± 1.0 pA, and 1.6 ± 2.4 pA; +Cre/+Flp was significantly different from baseline ($p = 0.0005$, Wilcoxon signed rank t-test).

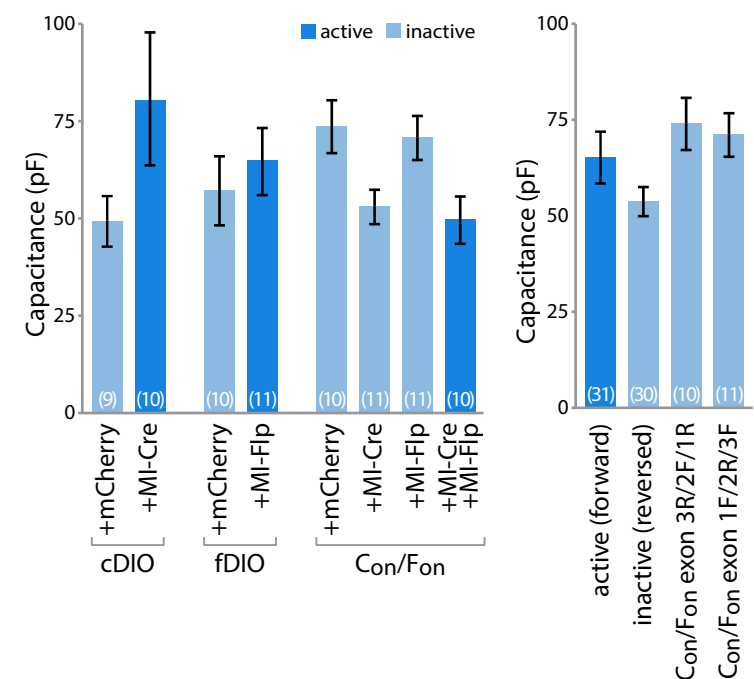
a



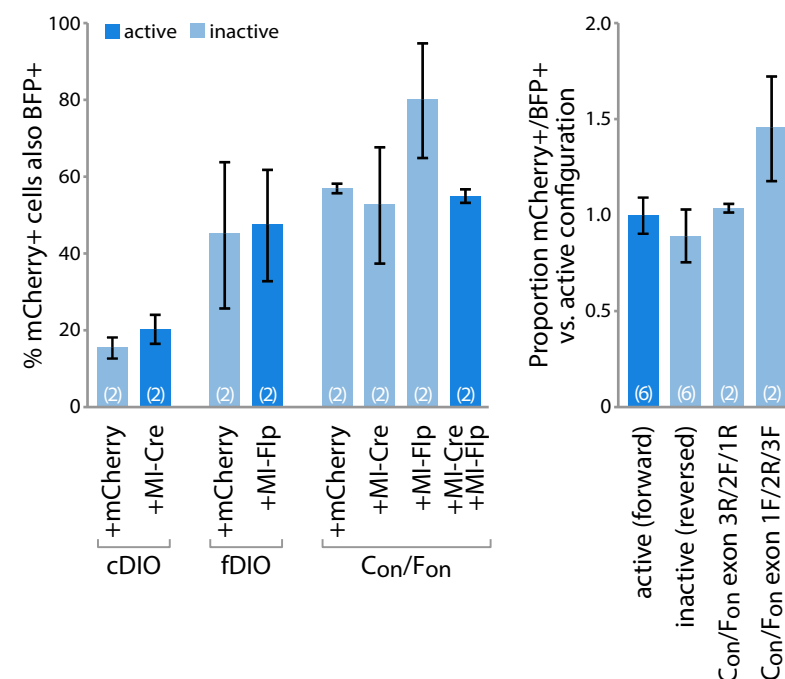
b



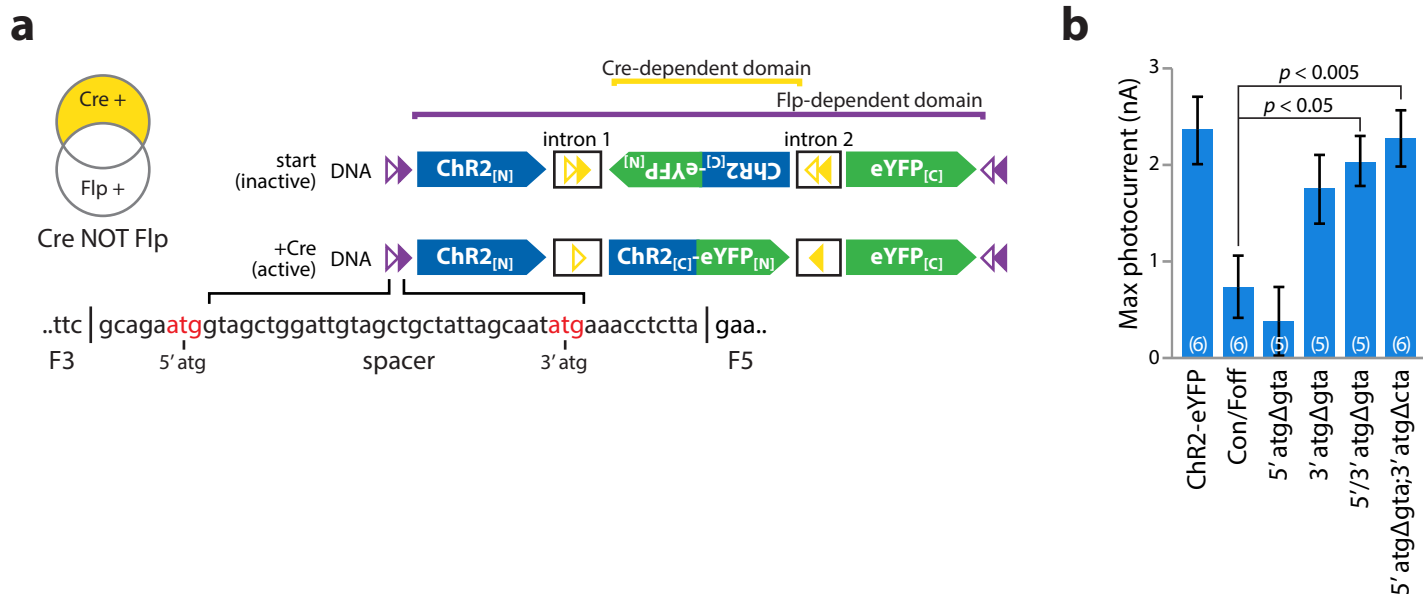
c



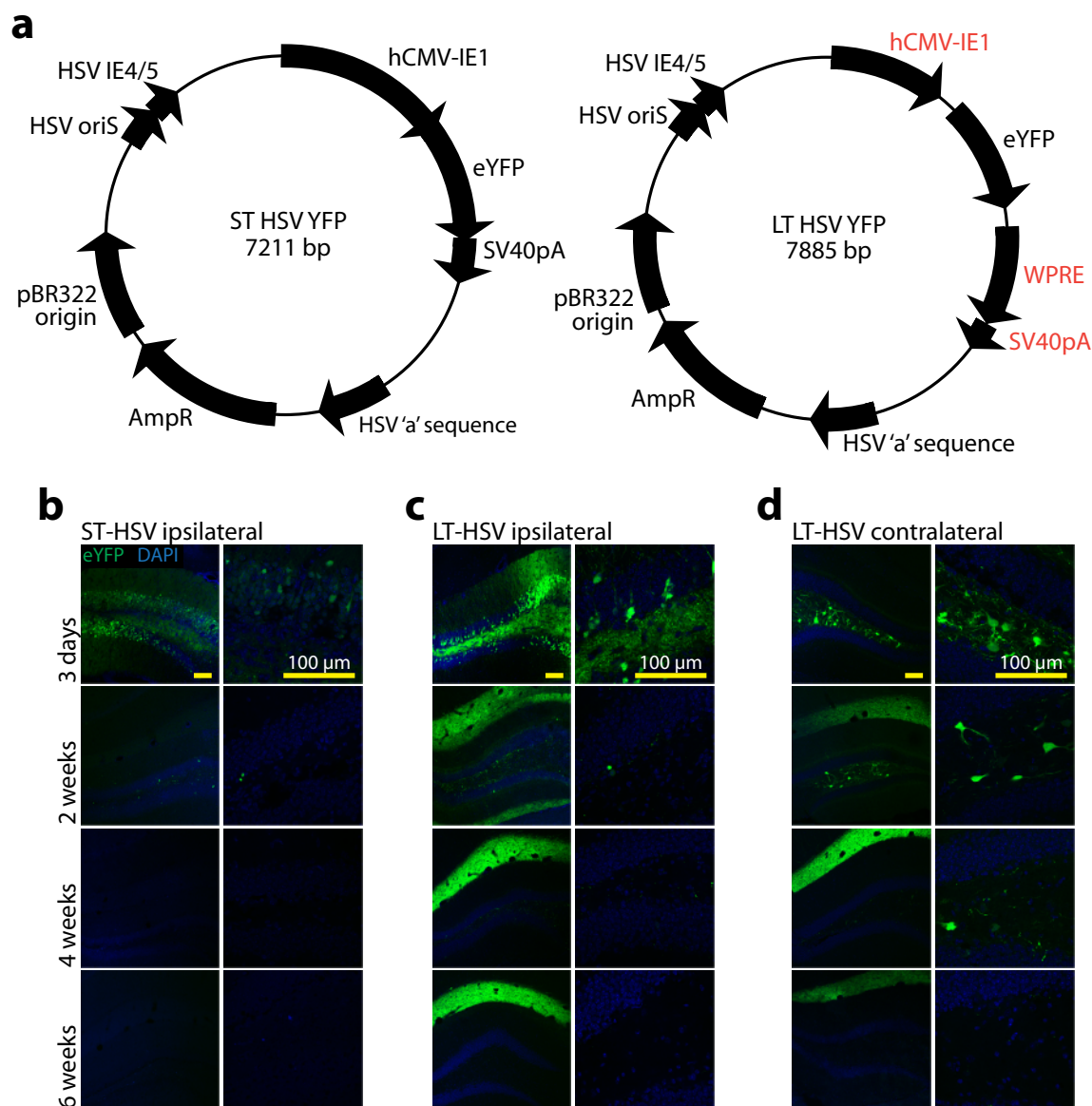
d



Supplementary Figure 10. Expressing recombinase-dependent constructs in non-active configurations does not influence membrane properties or viability. **a**) mCherry-tagged recombinases or mCherry were co-transfected with modified variants of fDIO-ChR2-YFP, cDIO-ChR2-eYFP, or Con/Fon-ChR2-eYFP that contain an independently-expressed blue fluorophore to assist in identifying neurons containing non-active recombinase-dependent constructs. **b,c**) No detrimental effect to either **(b)** input resistance or **(c)** capacitance of neurons expressing non-active recombinase-dependent constructs, either grouped by construct (*left*) or by ORF configuration (*right*) was observed. **d**) All recombinase/construct pairings were observed to have similar transfection rates (although an increase in cell number was observed for Con/Fon-ChR2-eYFP+MI-Cre+MI-Flp vs. Con/Fon-ChR2-eYFP+MI-Flp) either grouped by construct (*left*) or ORF configuration (*right*).

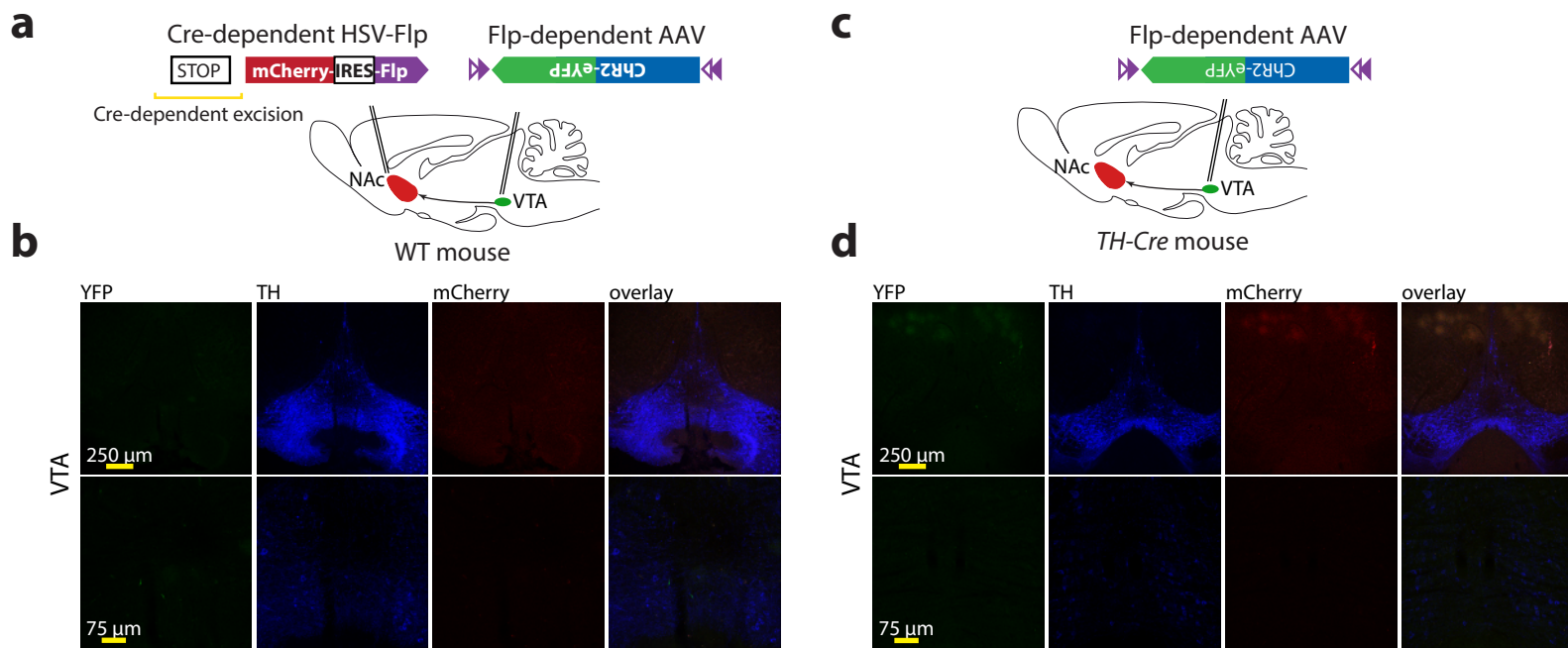


Supplementary Figure 11. Modification of the recombinase recognition sequence spacer region improves functional expression of Con/Foff-ChR2-eYFP. **a)** Con/Foff-ChR2-eYFP is expressed in neurons that exclusively express Cre recombinase and retains a complete fDIO recombinase recognition cassette in the active configuration, which contains two potential start codons (ATG). **b)** Combined mutations of the 3' and 5' ATG were sufficient to significantly increase photocurrents in Con/Foff-ChR2-eYFP relative to the ATG-containing spacer region (ChR2: 2368.7 ± 348.7 pA n=6, Con/Foff: 735.0 ± 328.1 pA n=6, 5' atgΔgta: 381.0 ± 356.8 pA n=5, 3' atgΔgta: 1758.0 ± 359.0 pA n=5, 5'/3' atgΔgta: 2032.1 ± 260.1 pA n=5, 5' atgΔgta;3' atgΔcta: 2273.6 ± 294.0 pA n=6; $p < 0.05$ Bonferroni's Multiple Comparison test $p < 0.05$ Con/Foff vs. 5'/3' atgΔgta, $p < 0.005$ Con/Foff vs. 5' atgΔgta;3' atgΔcta).



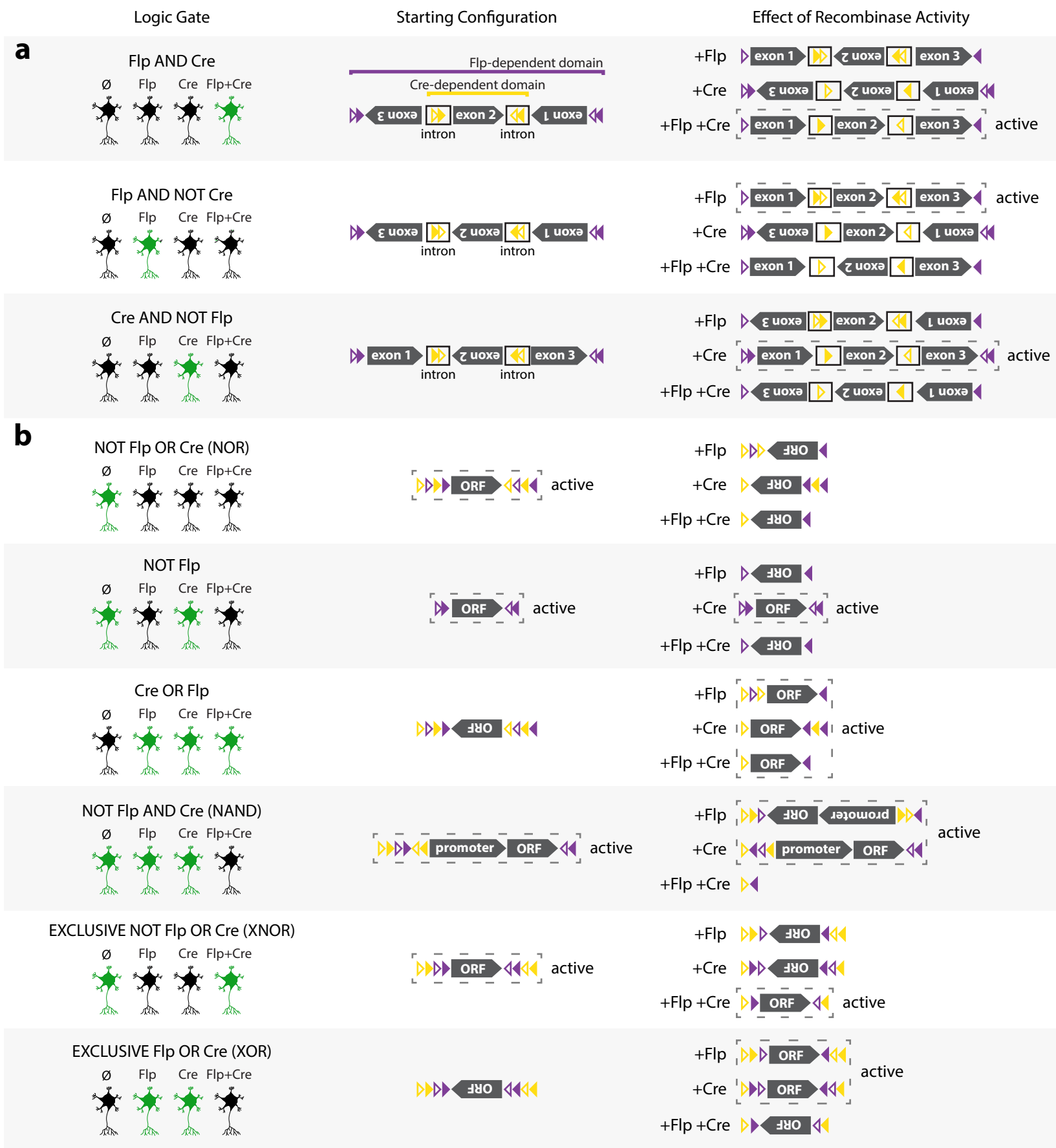
Supplementary Figure 13. In vivo expression time-series and eYFP activation from ST- and LT-HSV. **a)** Construct maps for ST- and LT-HSV-CMV-eYFP (EF1 α promoter in LT-HSV was used for targeting experiments in main figures). **b-d):** Virus (ST- or LT-HSV-CMV-eYFP) was injected unilaterally in dentate gyrus of adult (3-5 month old) mice, and imaged at time-points ranging from 3 days to 6 weeks. Data were obtained from 2 mice for each time-point, with the exception of the later (non-expressing) time-points for ST-HSV, for which only 1 mouse was used per time-point. ST- and LT-HSV were titer-matched (at 3×10^8 infectious units per mL) and confocal settings were matched across all conditions. **b)** Virus expression (green) at the injection site for ST-HSV-CMV-eYFP, at low (*left*) and high (*right*) magnification. Cell body expression was seen mainly in the granule cells at the earliest time-point, but disappeared after ~ 2 weeks. No expression was observed contralaterally at any time-point (data not shown). Cell bodies are labeled by DAPI (blue). **c)** Expression at the injection site for LT-HSV-CMV-eYFP, at low (*left*) and high (*right*) magnification. Cell body expression was seen mainly in the granule cells at the earliest time-point, but disappeared after ~ 2 weeks. Axonal expression in the molecular layer developed by the 2-week time-point and persisted through 6 weeks. **d)** Expression in the contralateral DG for LT-HSV-CMV-eYFP, at low (*left*) and high (*right*) magnification. Cell body expression was seen mainly in the hilar cells at the earliest time-point, but decreased over time, disappearing by 6 weeks. Axonal expression in the molecular layer developed by the 2-week time-point and persisted through 6 weeks. Confocal settings were matched across all conditions.

Supplementary Figure 14 - INTRASECT: single-component targeting of cells using multiple-feature Boolean logic



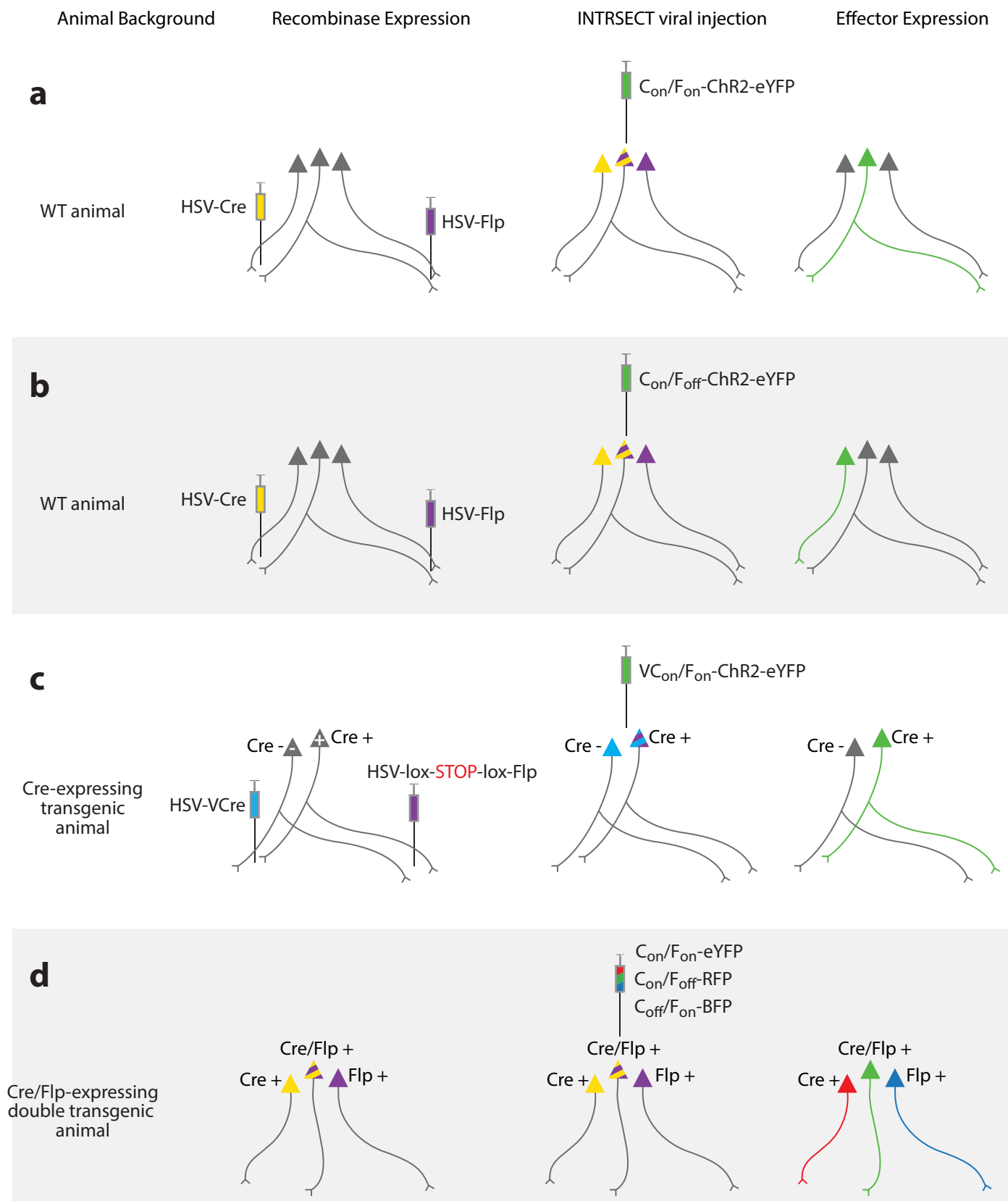
Supplementary Figure 14. Control data for combinatorial targeting with multiplexed recombinases: beyond genetic properties. **a)** Injection strategy for Cre-negative control. Cre-dependent Flp recombinase packaged in retrograde LT-HSV and Flp-dependent (fDIO) AAV-ChR2-eYFP were injected into the NAcc and VTA of a wild type mouse, respectively. **b)** *In vivo* expression pattern in the VTA, showing no eYFP expression as expected. **c)** Injection strategy for Flp-negative control. A Flp-dependent (fDIO) AAV-ChR2-eYFP was injected into the VTA of a *TH-IRES-Cre* mouse. **d)** *In vivo* expression pattern in the VTA, showing minimal eYFP expression.

Supplementary Figure 15 - INTRSECT: single-component targeting of cells using multiple-feature Boolean logic



Supplementary Figure 15. Diversity of INTRSECT-based logical operations. In addition to targeting cells that express a single recombinase exclusively or only cells expressing two recombinases (**a**; green cells), Cre and Flp may be used together to achieve additional expression patterns (**b**; ‘Logic Gate’) by changing the initial relative configuration/position of the ORF and recombinase recognition sites (‘Starting Configuration’) to direct response of the construct in response to recombinases (‘Effects of Recombinase Activity’). Active configurations denoted by dashed boxes. Note that NOR may also be achieved using intron-based multiple recombinase configuration.

Supplementary Figure 16 - INTRSECT: single-component targeting of cells using multiple-feature Boolean logic



Supplementary Figure 16. Combinatorial INTRSECT approaches. These multiple recombinase-dependent constructs may be combined with retrograde viral delivery of recombinases to target cells based on multiple traits. **a,b**) Viral delivery of Cre and Flp may be achieved using HSV tools described in this manuscript and may be combined with upstream delivery of AAV-DJ-Con/F_{off}-Chr2-eYFP in order to specifically express a genetic tool within neurons with collateralized projections (**a**) or to exclude a population of neurons projecting to multiple defined downstream locations (**b**). **c**) Transgenic animals expressing Cre within a defined locus are able to extend targeting control to include cells that both project to multiple defined loci AND have a specified genetic background. **d**) Last, a palette of injected viruses may be used to elucidate the expression patterns of multiple neuron subtypes using simultaneous injection of both AND as well as NOT conditional viruses controlling expression of various fluorophores.